FGFR3 Mutational Activation Can Induce Luminal-like Papillary Bladder Tumor Formation and Favors a Male Sex Bias

Ming-Jun Shi, Jacqueline Fontugne, Aura Moreno-Vega, Xiang-Yu Meng, Clarice Groeneveld, Florent Dufour, Aurélie Kamoun, Sia Viborg Lindskrog, Luc Cabel, Clémentine Krucker, et al.

available at www.sciencedirect.com
journal homepage: www.europeanurology.com

European Association of Urology

Bladder Cancer

FGFR3 Mutational Activation Can Induce Luminal-like Papillary Bladder Tumor Formation and Favors a Male Sex Bias

Ming-Jun Shi [a,b,c,†], *Jacqueline Fontugne* [b,c,d,e,†], *Aura Moreno-Vega* [b,c,†], *Xiang-Yu Meng* [b,c,f,†], *Clarice Groeneveld* [b,g,†], *Florent Dufour* [b,c,h], *Aurélie Kamoun* [g], *Sia Viborg Lindskrog* [i], *Luc Cabel* [b,c], *Clémentine Krucker* [b,c], *Audrey Rapinat* [j], *Claire Dunois-Larde* [b,c], *May-Linda Lepage* [b,c], *Elodie Chapeaublanc* [b,c], *Olivier Levrel* [k], *Victoria Dixon* [b,e], *Thierry Lebret* [l], *Anna Almeida* [j], *Aurélien De Reynies* [g], *Natacha Rochel* [m,n,o,p], *Lars Dyrskjøt* [i], *Yves Allory* [b,d,e], *François Radvanyi* [b,c], *Isabelle Bernard-Pierrot* [b,c,*]

[a] *Department of Urology, Beijing Friendship Hospital, Capital Medical University, Beijing, China;* [b] *Institut Curie, PSL Research University, CNRS, UMR144, Equipe Labellisée Ligue contre le Cancer, Paris, France;* [c] *Sorbonne Universités, UPMC Université Paris 06, CNRS, UMR144, Paris, France;* [d] *Université Versailles St-Quentin, Université Paris-Saclay, Montigny-le-Bretonneux, France;* [e] *Institut Curie, Department of Pathology, Saint-Cloud, France;* [f] *Department of Urology, Zhongnan Hospital of Wuhan University, Wuhan, China;* [g] *La Ligue contre le Cancer, Paris, France;* [h] *Inovarion, Paris, France;* [i] *Department of Molecular Medicine, Aarhus University Hospital, Aarhus, Denmark;* [j] *Department of Translational Research, Institut Curie, Paris, France;* [k] *MEDIPATH Les Jalassières, Eguilles, France;* [l] *Service d'Urologie, Hôpital Foch, Suresnes, France;* [m] *Institut de Génétique et de Biologie Moléculaire et Cellulaire (IGBMC), Illkirch, France;* [n] *Institut National de La Santé et de La Recherche Médicale (INSERM), Illkirch, France;* [o] *U1258/Centre National de Recherche Scientifique (CNRS), Illkirch, France;* [p] *UMR7104/Université de Strasbourg, Illkirch, France*

Article info

Article history:
Accepted September 29, 2022

Associate Editor:
James Catto

Keywords:
Bladder cancer
Fibroblast growth factor receptor 3
Androgen receptor
Estrogen receptor
Sex bias
Mouse model
Luminal tumors
Tyrosine kinase receptor

Abstract

Background: Bladder cancer (BCa) is more common in men and presents differences in molecular subtypes based on sex. Fibroblast growth factor receptor 3 (*FGFR3*) mutations are enriched in the luminal papillary muscle-invasive BCa (MIBC) and non-MIBC subtypes.
Objective: To determine whether *FGFR3* mutations initiate BCa and impact BCa male sex bias.
Design, setting, and participants: We developed a transgenic mouse model expressing the most frequent *FGFR3* mutation, FGFR3-S249C, in urothelial cells. Bladder tumorigenesis was monitored in transgenic mice, with and without carcinogen exposure. Mouse and human BCa transcriptomic data were compared.
Intervention: Mutant *FGFR3* overexpression in mouse urothelium and siRNA knockdown in cell lines, and N-butyl-N(4-hydroxybutyl)-nitrosamine (BBN) exposure.
Outcome measurements and statistical analysis: Impact of transgene dosage on tumor frequency, synergy with BBN treatment, and FGFR3 pathway activation were analyzed. The sex-specific incidence of *FGFR3*-mutated tumors was evaluated in mice and humans. *FGFR3* expression in FGFR3-S249C mouse urothelium and in various human epithelia

† These authors contributed equally to the work.
* Corresponding author. Institut Curie, 26 rue d'Ulm, 75005 Paris, France. Tel. +33 1 42 34 63 40; Fax: +33 1 42 34 63 49.
E-mail address: ibernard@curie.fr (I. Bernard-Pierrot).

https://doi.org/10.1016/j.eururo.2022.09.030

Please cite this article as: M.-J. Shi, J. Fontugne, A. Moreno-Vega et al., FGFR3 Mutational Activation Can Induce Luminal-like Papillary Bladder Tumor Formation and Favors a Male Sex Bias, Eur Urol (2022), https://doi.org/10.1016/j.eururo.2022.09.030

Tumor microenvironment

was measured. Mutant *FGFR3* regulation of androgen (*AR*) and estrogen (*ESR1*) receptor activity was evaluated, through target gene expression (regulon) and reporter assays.

Results and limitations: FGFR3-S249C expression in mice induced low-grade papillary BCa resembling human luminal counterpart at histological, genomic, and transcriptomic levels, and promoted BBN-induced basal BCa formation. Mutant FGFR3 expression levels impacted tumor incidence in mice, and mutant *FGFR3*–driven human tumors were restricted to epithelia presenting high normal *FGFR3* expression levels. BCa male sex bias, also found in our model, was even higher in human *FGFR3*-mutated tumors compared with wild-type tumors and was associated with higher AR and lower ESR1 regulon activity. Mutant *FGFR3* expression inhibited both ESR1 and AR activity in mouse tumors and human cell lines, demonstrating causation only between FGFR3 activation and low ESR1 activity in tumors.

Conclusions: Mutant *FGFR3* initiates luminal papillary BCa formation and favors BCa male sex bias, potentially through FGFR3-dependent ESR1 downregulation. Patients with premalignant lesions or early-stage BCa could thus potentially benefit from FGFR3 targeting. *FGFR3* expression level in epithelia could account for FGFR3-driven carcinoma tissue specificity.

Patient summary: By developing a transgenic mouse model, we showed that gain-of-function mutations of *FGFR3* receptor, among the most frequent genetic alterations in bladder cancer (BCa), initiate BCa formation. Our results could support noninvasive detection of *FGFR3* mutations and FGFR3 targeting in early-stage bladder lesions.

1. Introduction

Bladder cancer (BCa) is the sixth most common cancer in men worldwide [1]. At diagnosis, most tumors are non–muscle-invasive urothelial carcinomas (NMIBC; 75%). NMIBCs have a high recurrence rate (70%), and a subset (10–15%) progresses to the aggressive form of disease—muscle-invasive bladder cancer (MIBC). Molecular classifications have been established in both NMIBC and MIBC to identify different biological processes to support patient treatment stratification [2–7].

Fibroblast growth factor receptor 3 (FGFR3), a receptor tyrosine kinase, is frequently genetically altered in BCa [3,5,8,9]. Point mutations (observed in 70% of NMIBCs and enriched in classes 1 and 3, and in 15% of MIBCs, mostly in the luminal papillary [LumP] subtype [2–7]) or chromosomal translocations resulting in protein fusions (affecting 5% of MIBCs) lead to a constitutively active FGFR3. The transforming properties of genetically altered *FGFR3* have been shown in vitro, and FGFR3 oncogenic dependency for tumor growth has been demonstrated both in vitro and in vivo [10–14]. Recently, the FGFR inhibitor erdafitinib received US Food and Drug Administration approval for patients with locally advanced or metastatic BCa with *FGFR3/2* alterations [15].

To determine the functional role of *FGFR3* mutations in BCa in vivo, several teams have developed *FGFR3*-altered genetically engineered mice (GEMs) through transgene insertion (mouse mutant K644E [16] or S243C [17], and human S249C [18]). So far, results suggest that FGFR3 activation alone is not sufficient to induce tumorigenesis [16,18,19], but can promote tumor formation when associated with other molecular alterations (p53/pRB deficiency [17] or PTEN loss [19]) or with carcinogen treatment [18].

Here, we report for the first time a GEM model overexpressing the human *FGFR3*b-S249C mutant in the urothelium, in which mice develop low-grade papillary BCa, resembling the human counterpart at histological, genomic, and transcriptomic levels. The impact of FGFR3-S249C expression on tumor formation penetrance led us to investigate *FGFR3* expression levels in different normal human epithelia and its role in the tissue specificity of *FGFR3*-driven tumors. The higher incidence of tumors in male mice prompted us to explore sex distribution and to investigate sex hormone receptors (androgen receptor [AR] and estrogen receptor 1 [ESR1]) activation in *FGFR3*-mutated human BCa and cell lines.

2. Materials and methods

All the materials and methods are described in the Supplementary material.

3. Results

3.1. *FGFR3-S249C expression in uroplakin II–expressing cells induces urothelial hyperplasia and low-grade papillary NMIBC*

We generated transgenic mice expressing a human mutant *FGFR3* in the urothelium. We focused on the most common *FGFR3* mutation in both NMIBC and MIBC, S249C [8], and used the mouse uroplakin II (UII) gene promoter to specifically target its expression to urothelial cells (Fig. 1A) [20]. We selected two founders for our UII-hFGFR3-S249C model, numbers 569 and 538, which expressed high levels of the transgene in the urothelium (mostly in the suprabasal and intermediate cell layers; Supplementary Fig. 1). These two founders were viable and fertile, and transmitted the transgene to their offspring in a Mendelian fashion. Following the

Please cite this article as: M.-J. Shi, J. Fontugne, A. Moreno-Vega et al., FGFR3 Mutational Activation Can Induce Luminal-like Papillary Bladder Tumor Formation and Favors a Male Sex Bias, Eur Urol (2022), https://doi.org/10.1016/j.eururo.2022.09.030

propagation of founder lines, we examined the bladder of heterozygous or homozygous transgenic mice (one or two alleles of the transgene, respectively) aged 1–18 mo. Macroscopically, papillary lesions were observed in both lines after 15 mo. Tumor incidence was further studied in mouse 569 line, which showed higher hFGFR3-S249c expression level and higher phenotype penetrance. The overall penetrance at 18 mo was low (~10%), and tumor incidence was impacted by both sex and zygosity (Fig. 1B). Males developed more tumors than females, and homozygous mice developed more tumors than heterozygous mice in both sexes. The tumors corresponded histologically to NMIBCs (stage pTa) of papillary architecture with exophytic or mixed (exophytic and inverted) growth patterns and low-grade cytological atypia (Fig. 1C). Similar to human low-grade pTa BCa, mouse tumor proliferation rate was low, with <5% of Ki67-labeled nuclei by immunohistochemistry (Fig. 1D). A systematic histological analysis of UII-hFGFR3-S249C mice bladders also identified hyperplastic lesions, defined by a thickened urothelium without cytological atypia, with an increase to up to 20 cell layers (Fig. 1C). The penetrance of the hyperplastic phenotype was complete from 6 mo of age in both lines.

3.2. *FGFR3-induced mouse tumors harbor copy number alterations and transcriptomic modulation of hallmark cancer pathways*

We performed genomic and transcriptomic characterization of tumors obtained from line 569. Whole-exome sequencing did not reveal any recurrent mutations but showed recurrent copy number alterations (CNAs), the most common being chromosome 16 gains in five out of seven sequenced tumors (Fig. 2A). We confirmed the chromosomal gains by quantitative polymerase chain reaction (qPCR) of three selected genes of gained regions (*Trat1*, *Erbb4*, and *Fkbp5* located inchr16, chr1, and chr17, respectively) in six sequenced tumors and four additional tumors (Supplementary Fig. 2A), but not in hyperplasia (n = 6; Supplementary Fig. 2B). Gene expression profiles of hyperplastic lesions (n = 6) from UII-hFGFR3-S249C mice were more similar to normal samples (n = 3 control littermate urothelia) than tumors (n = 6) in the principal component analysis (Fig. 2B). Fewer than 200 significantly differentially expressed genes (DEGs) were found between hyperplasia and normal controls (Fig. 2C and Supplementary Table 1). In contrast, 1118 DEGs were identified between hFGFR3-S249C mouse tumors and controls (Fig. 2C and Supplementary Table 1). Furthermore, genes dysregulated in hyperplasia were enriched in the DEGs found in tumors (Fig. 2D).

A gene set enrichment analysis using DEGs in mouse tumors and hyperplasia (when compared with controls) and upon FGFR3 siRNA knockdown in human FGFR3-dependent BCa cell lines (see DEGs in Supplementary Tables 1 and 2) highlighted common enriched pathways (with NES in opposite directions), suggesting direct FGFR3 modulation. Specifically, we identified an increase in "cell cycle" and "DNA replication," and a decrease of "inflammation" and "interferon gamma" terms (Fig. 2E and Supplementary Table 3). Alterations in "mitotic spindle" and "sister chromatid segregation" pathways (Fig. 2E) could contribute to CNAs observed in FGFR3-S249C–induced tumors (Fig. 2A). As previously demonstrated in human BCa, MYC activation could also contribute to FGFR3 oncogenic properties in mice (Fig. 2E) [14]. Further supporting an FGFR3-dependent alteration of cell cycle regulation, a Western blot analysis showed a decrease in p27 and p53 expression in hyperplasia and tumors from UII-hFGFR3-S249C mice compared with the normal urothelium from controls (Fig. 2F). Of note, no recurrent mutations of *TP53* were observed in mice tumors.

3.3. *UII-hFGFR3-S249C model is a model of human luminal papillary BCa, but BBN-induced tumors in UII-hFGFR3-S249C mice retain a basal/squamous phenotype*

We and others have previously shown that N-butyl-N(4-hydroxybutyl) nitrosamine (BBN)-induced bladder tumors in mice represent a model of the basal subtype of MIBC [21–23]. Given the papillary nature of hFGFR3-S249C–induced murine tumors, we hypothesized that these recapitulate the LumP consensus subtype of human BCa, which is enriched in *FGFR3* mutations.

We first identified genomic-level similarities, with a significant overlap in genes with CNAs between the mouse model and human pTa *FGFR3*-mutated tumors (our CIT cohort, n = 44; Fig. 3A) [24]. Then, we classified hFGFR3-S249C tumors (n = 6) using a recently proposed NMIBC transcriptomic classifier [7]. The hFGFR3-S249C–induced tumors showed high correlations with NMIBC class 1 and 3 centroids, which are classes enriched in *FGFR3* mutations in humans (Fig. 3B) [5,7]. Using the BASE47 classifier [25], *FGFR3*-induced mice tumors were defined as luminal, whereas previously obtained BBN-induced tumors [21] were classified as basal (Fig. 3C). To further validate these findings, we performed a cross-species comparison by coclustering hFGFR3-S249C and BBN mice tumors with human tumors from our CIT-BLCA cohort (n = 96 MIBCs and 99 NMIBCs) [24], using corresponding orthologues of genes from the consensus classifier for the basal/squamous (Ba/Sq), LumP, and neuroendocrine-like subtypes [2]. BBN mice tumors clustered with human Ba/Sq tumors and hFGFR3-S249C with LumP human tumors (Fig. 3D).

We confirmed, as previously described [18], that hFGFR3-S249C expression promoted BBN-induced carcinogenesis (Supplementary Fig. 3A and 3B). Of note, BBN-induced FGFR3-mutated tumors retained Ba/Sq features, with frequent squamous differentiation and similar immunohistochemical expression patterns to that of BBN-induced tumors from littermate control mice, when considering basal marker CK5/6 and luminal marker FOXA1 (Supplementary Fig. 3C).

Human FGFR3-mutated tumors are characterized by low immune infiltration compared with other subtypes [2,5,7]. In line with this observation, a comparison of mouse tumor immune population abundance, inferred with the murine Microenvironment Cell Population counter (mMCP-counter) [26], with that of The Cancer Genome Atlas (TCGA)

Please cite this article as: M.-J. Shi, J. Fontugne, A. Moreno-Vega et al., FGFR3 Mutational Activation Can Induce Luminal-like Papillary Bladder Tumor Formation and Favors a Male Sex Bias, Eur Urol (2022), https://doi.org/10.1016/j.eururo.2022.09.030

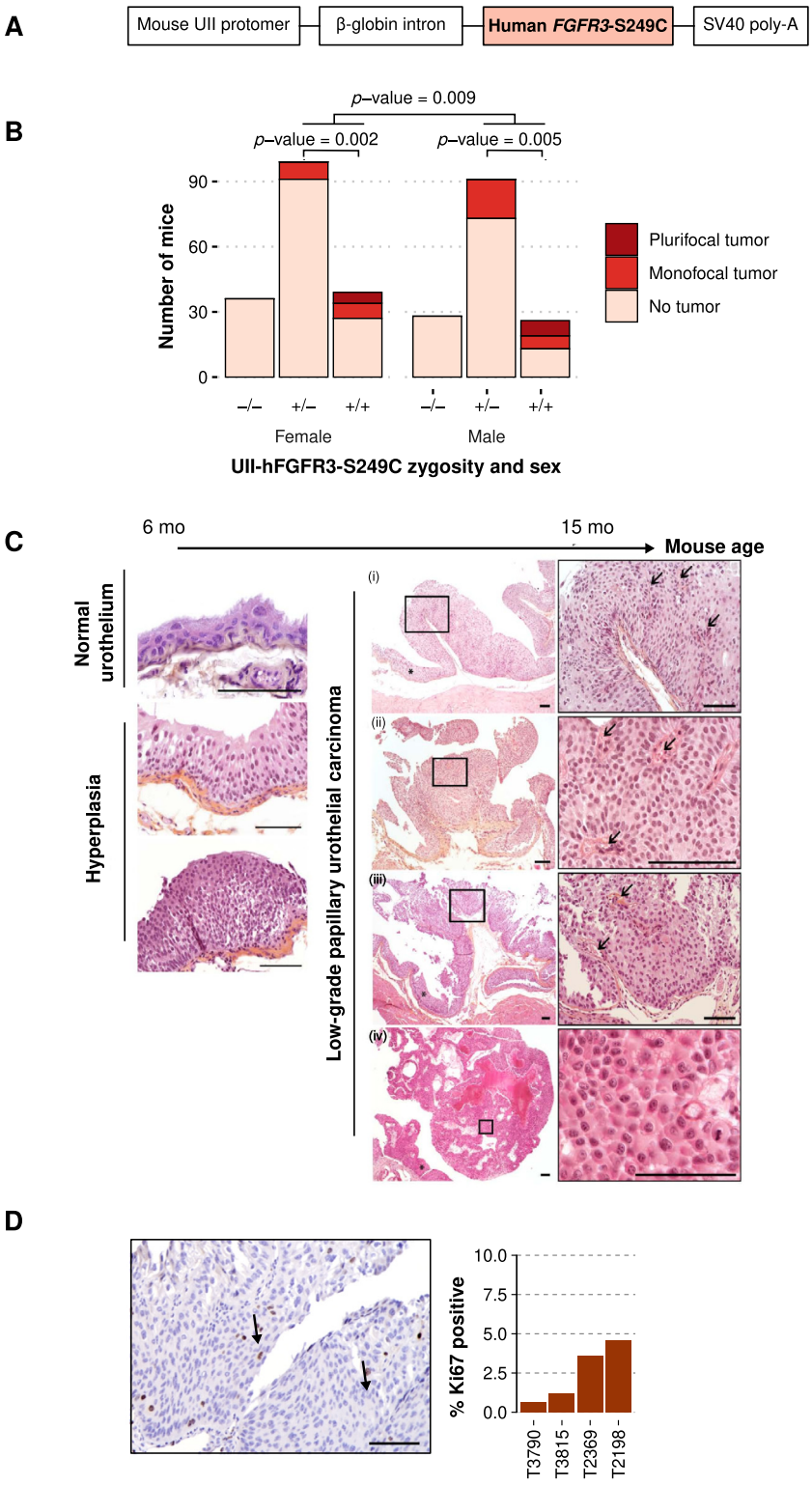

Fig. 1 – UPII-FGFR3-S249C transgenic mice develop urothelial hyperplasia and non–muscle-invasive low-grade urothelial carcinoma. (A) Chimeric construct used to generate transgenic mice, consisting of a 3.6-kb mouse *UPII* gene promoter and a 2.1-kb human *FGFR3b* cDNA carrying the mutation S249C. (B) Frequency of mono- or plurifocal bladder tumor development in homozygous (+/+) or heterozygous (+/–) hFGFR3-S249C mice versus control littermates (–/–) at 18 mo. Proportions of mice developing either mono- or plurifocal tumors between homozygous (+/+) and heterozygous (+/–) mice were compared using Fisher's exact tests within each sex. We also found that male mice developed more tumors than female tumors, controlling for zygosity, using a Cochran-Mantel-Haenszel chi-square test. (C) Representative H&E histology of urothelial lesions in hFGFR3-S249C mice compared with normal mouse urothelium. Hyperplastic lesions (left panel) or low-grade papillary urothelial carcinomas (right panel) developed in hFGFR3-S249C mice from 6 or 15 mo of age, respectively. Asterisks show tumor-adjacent urothelial hyperplasia. Arrows point to papillae fibrovascular cores. Scale bar: 100 μm. (D) Ki67 staining of hFGFR3-S249C mouse tumors. A representative stained slide is shown on the left; arrows indicate Ki67-positive cells. The proportion of Ki67-positive tumor cells was evaluated in four tumors; all were classified as low grade with <5% Ki67-positive cells. Scale bar: 100 μm. FGFR3 = fibroblast growth factor receptor 3; H&E = hematoxylin and eosin; UII = uroplakin II.

Please cite this article as: M.-J. Shi, J. Fontugne, A. Moreno-Vega et al., FGFR3 Mutational Activation Can Induce Luminal-like Papillary Bladder Tumor Formation and Favors a Male Sex Bias, Eur Urol (2022), https://doi.org/10.1016/j.eururo.2022.09.030

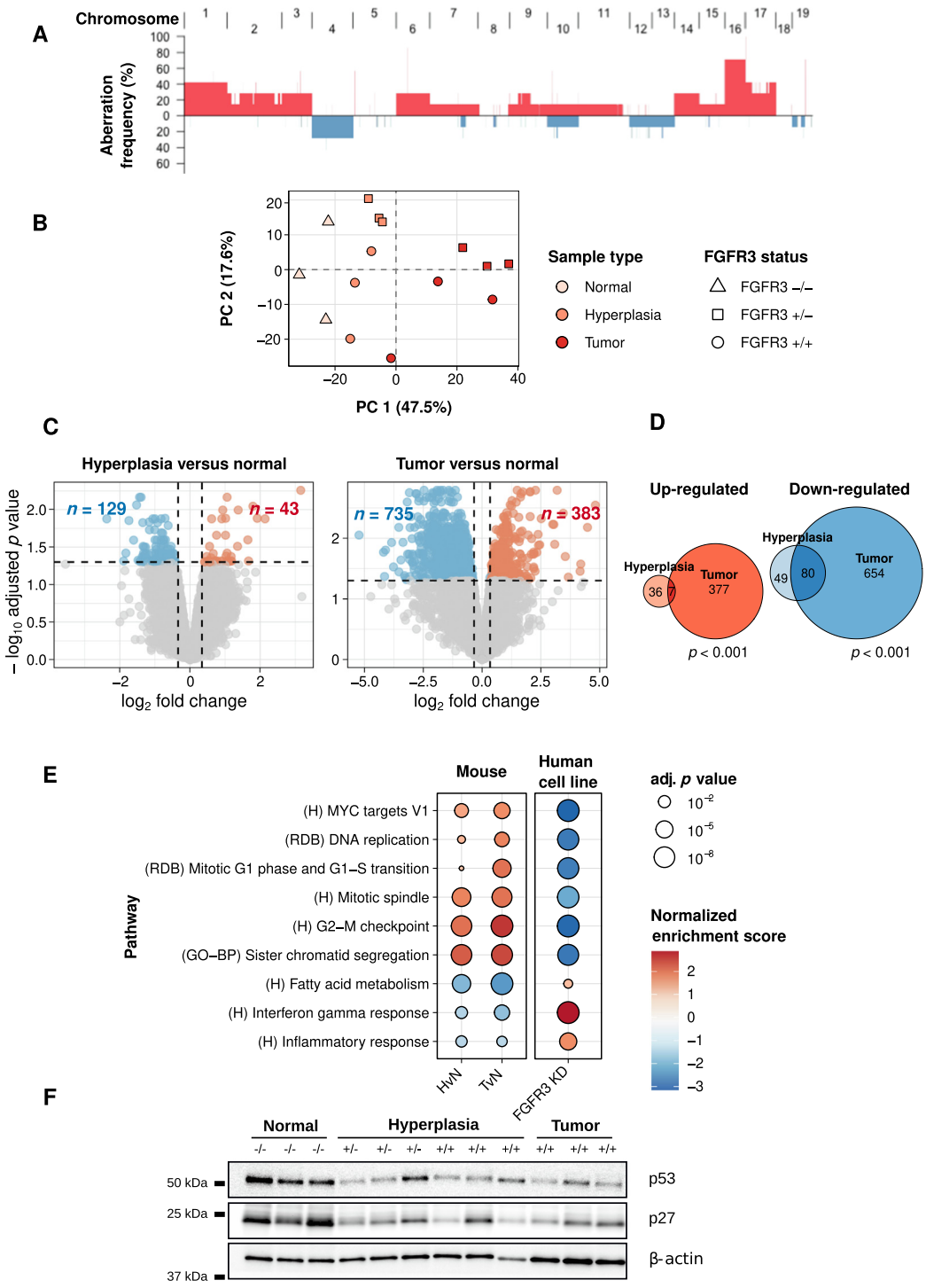

Fig. 2 – Mouse hFGFR3-S249C tumors present copy number alterations and transcriptomic modulation of some key cancer hallmarks pathways. (A) Frequency of chromosomal copy number alterations in UII-hFGFR3-S249C tumors. (B) Principal component analysis of the 1000 most varying genes expressed on the Affymetrix Mouse Exon 1.0 ST array from tumor, and hyperplastic urothelium from UPII-hFGFR3-S249C mice and normal urothelial samples from control littermates. (C) Volcano plot of the differentially expressed genes (|log2FC| > 0.35; adj. $p < 0.05$) between hFGFR3-S249C mice hyperplasia and littermate normal control urothelia (left panel, 172 DEGs) and between hFGFR3-S249C mice tumors and controls (right panel, 1118 DEGs). Lists of DEGs are provided in Supplementary Table 1. (D) Comparison of up- and downregulated genes between hFGFR3-S249C hyperplastic urothelium and normal urothelium from littermates (controls) and hFGFR3-S249C tumors versus controls. Overlap was evaluated using Fisher's exact test. (E) Gene set enrichment analysis of deregulated pathways in (left) hFGFR3-S249C hyperplastic urothelium compared with normal urothelium from control littermates (HvN), (center) hFGFR3-S249 tumors compared with controls (TvN), and (right) *FGFR3* knockdown compared with control in three *FGFR3*-dependent bladder cancer cell lines (RT-112, UM-UC-14, and MGH-U3). Normalized enrichment scores and FDRs of curated significantly enriched terms are displayed. A list of DEGs in cell lines is provided in Supplementary Table 2. (F) Western blot analysis of p53 and p27 protein levels in normal urothelium of control littermate mice and in hyperplastic urothelium and bladder tumors from either heterozygous (+/–) or homozygous (+/+) hFGFR3-S249C mice. B-actin was used as loading control. DEG = differentially expressed gene; FDR = false discovery rate; FGFR3 = fibroblast growth factor receptor 3; UII = uroplakin II.

Please cite this article as: M.-J. Shi, J. Fontugne, A. Moreno-Vega et al., FGFR3 Mutational Activation Can Induce Luminal-like Papillary Bladder Tumor Formation and Favors a Male Sex Bias, Eur Urol (2022), https://doi.org/10.1016/j.eururo.2022.09.030

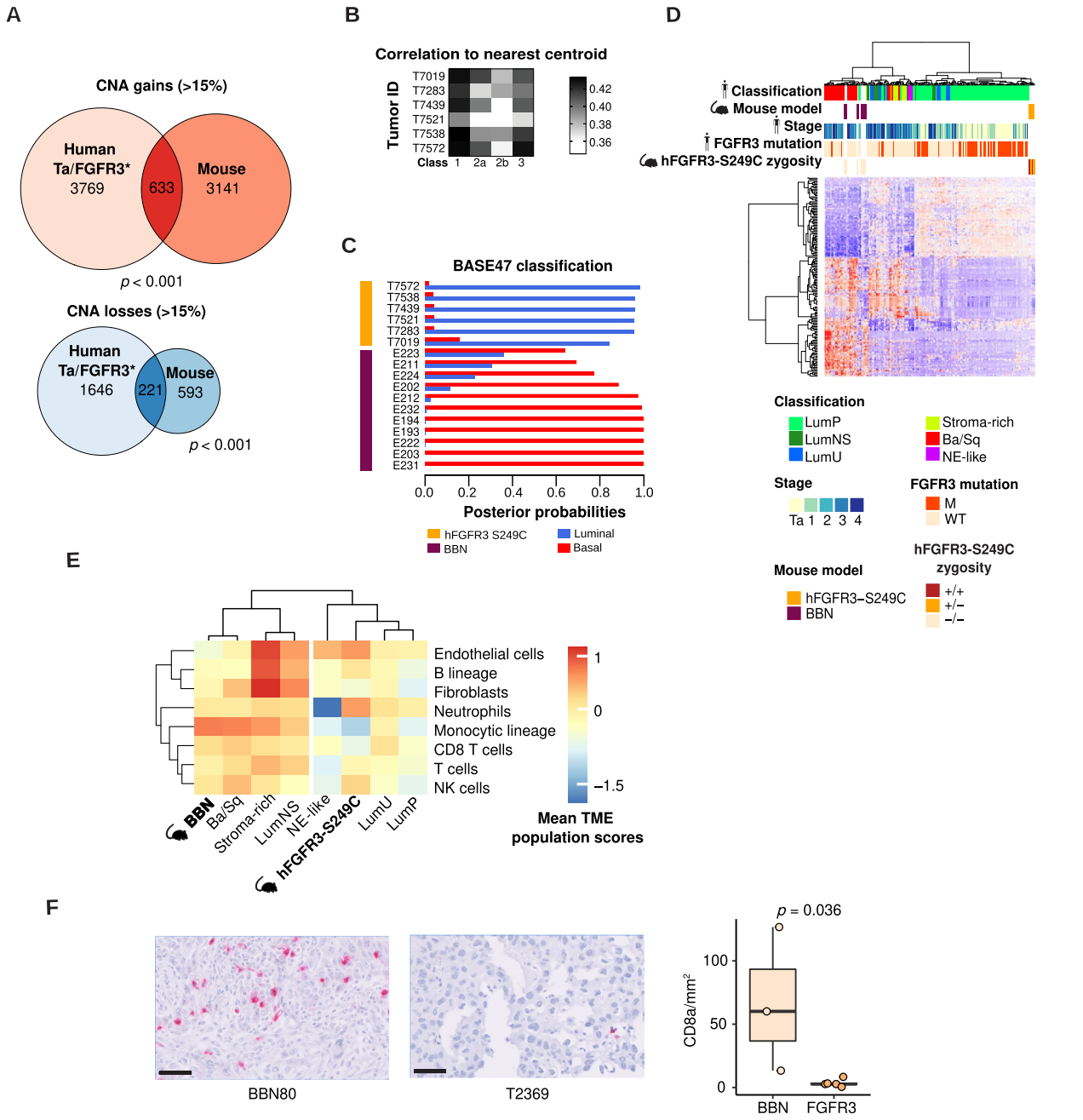

Fig. 3 – Mouse *hFGFR3*-S249C bladder tumors resemble human luminal papillary tumors. (A) Comparison of genes with frequent (>15%) copy number gains (top) and losses (bottom) between pTa *FGFR3*-mutated human tumors and *hFGFR3*-S249C mouse tumors. Overlap was evaluated using Fisher's exact tests. (B) Correlation with the nearest centroid of the four classes of UROMOL non–muscle-invasive carcinoma classification scheme [5,7] and (C) the BASE47 classifier [25] for tumors of *hFGFR3*-S249C mice. Muscle-invasive tumors derived from N-butyl-N-(4-hydroxybutyl)nitrosamine (BBN)-treated mice are used for comparison [21]. (D) Cross-species unsupervised hierarchical clustering of *hFGFR3*-S249C mice tumors (n = 6), BBN-induced tumors (n = 11), and human bladder tumors (n = 193 from the CIT series) considering genes from the consensus classifier for basal/squamous and luminal-papillary human BCa [2]. (E) Cross-species unsupervised hierarchical clustering using microenvironment cellular compositions estimated with mMCP-counter and MCP-counter scores, for BBN (n = 11) and *hFGFR3*-S249C (n = 6) models and TCGA MIBCs according to consensus subtype (n = 408). (F) Representative CD8 IHC staining (left panel) and quantification of CD8-positive lymphocytes per millimeter square of tumor surface in BBN-induced and *hFGFR3*-induced mouse bladder carcinoma (right panel). Differences were assessed using Wilcoxon rank-sum test. Ba/Sq = basal/squamous; BCa = bladder cancer; CNA = copy number alteration; FGFR3 = fibroblast growth factor receptor 3; IHC = immunohistochemical; LumNS = luminal nonspecified; LumP = luminal papillary; LumU = luminal unstable; MCP-counter = Microenvironment Cell Population counter; MIBC = muscle-invasive bladder cancer; mMCP-counter = murine Microenvironment Cell Population counter; NE-like = neuroendocrine-like; NK cell = natural killer cell; TCGA = The Cancer Genome Atlas; TME = tumor microenvironment.

MIBC tumors (n = 408), estimated with MCP-counter, found similar clustering results, suggesting that both BBN and FGFR3 models are relevant to study tumor microenvironment in basal and luminal bladder tumors, respectively (Fig. 3E). CD8a immunostaining confirmed these results (Fig. 3E), showing lower infiltration of CD8+ lymphocytes in FGFR3-mutated mice tumors than in BBN-induced mice tumors.

Please cite this article as: M.-J. Shi, J. Fontugne, A. Moreno-Vega et al., FGFR3 Mutational Activation Can Induce Luminal-like Papillary Bladder Tumor Formation and Favors a Male Sex Bias, Eur Urol (2022), https://doi.org/10.1016/j.eururo.2022.09.030

3.4. FGFR3 expression levels impact tumor formation in UII-hFGFR3-S249C mice and could account for tissue specificity of mutant FGFR3–induced tumors

We further explored the impact of hFGFR3-S249C zygosity on tumorigenesis, given the increased frequency and tumor multifocality in homozygous mice (Fig. 1B). We confirmed that the transgene expression was higher in the hyperplastic urothelium of homozygous mice than in that of heterozygous mice at mRNA and protein levels (Fig. 4A and 4B, respectively). The same difference was observed in tumors at the mRNA level (Fig. 4A). We also analyzed FGFR3 protein expression in tumors from homozygous mice and observed similar expression levels to the hyperplastic urothelium of homozygous hFGFR3-S249C mice (Fig. 4B). Using DEGs upon *FGFR3* knockdown in FGFR3-dependent BCa cell lines (Supplementary Table 2) and genes overexpressed in *FGFR3*-mutated MIBC tumors from the TCGA-BLCA cohort, we developed an FGFR3-activation signature (area under the curve = 0.9 for detecting *FGFR3*-mutated tumors in CIT data; Supplementary material and Supplementary Fig. 4). We observed a gradual increase in FGFR3 signature scores with gene dosage and tumor development stages (Fig. 4C and 4D). We therefore hypothesized that higher h*FGFR3* expression level in homozygous than in heterozygous mice urothelium (Fig. 4A and 4B) could increase tumor development susceptibility. We thus measured FGFR3b (main isoform expressed in epithelial cells) expression levels in different normal human epithelia, including the urothelium, obtained after laser microdissection. Interestingly, epithelia presenting high *FGFR3b* expression levels were those in which *FGFR3*-mutated tumors are described (bladder, skin, and exocervix; Fig. 4E) [3,27–29]. Our data suggest that high epithelial expression of *FGFR3* is required for *FGFR3* mutations to induce tumor formation. Nevertheless, although *FGFR3* gene dosage in mice influenced tumor frequency, it did not impact tumor latency or induce progression toward MIBC.

3.5. Mutant FGFR3 induces a higher BCa male sex bias and represses ESR1 transcriptional activity

BCa is a sex-biased cancer occurring three times more in men than in women [30]. The distribution of molecular subtypes is sex dependent, males being enriched with tumors of the LumP and neuroendocrine-like subtypes and females with the Ba/Sq subtype [31]. A male sex bias in luminal tumors induced by the constitute activation of β-catenin was also observed in mice [32]. Given the higher proportion of males developing *FGFR3*-S249C–induced tumors (Fig. 1B), we explored the relationship between sex and *FGFR3* mutation status in human tumors (Fig. 5A). Since *FGFR3* mutations other than S249C display the same or a higher oncogenic potential [8,30,31], we considered all *FGFR3* mutations and not only S249C for further analysis. Considering all tumors, we observed a significantly higher male/female ratio in *FGFR3*-mutated tumors than in *FGFR3* wild-type tumors (Fig. 5A). *FGFR3* mutation enrichment in males was driven by MIBCs, in particular by the LumP subtype, for which the male/female ratio was significantly higher (around 3.5-fold) in *FGFR3*-mutated than in *FGFR3* wild-type (not mutated) tumors. Class 3 NMIBCs also presented a trend for such a bias, albeit not significant, potentially due to low numbers of *FGFR3* wild-type tumors. These observations suggested that sex-specific pathways could synergize with *FGFR3* mutations to induce BCa, in particular in LumP MIBC. We thus investigated sex hormone receptor activation in association with *FGFR3* mutations. Using AR and ESR1 regulon gene sets defined for MIBC and NMIBC [2,7] and filtered for direct target genes using ChIP-seq data (Supplementary material), we calculated AR and ESR1 filtered regulon activity in both NMIBCs from UROMOL and MIBCs from TCGA cohorts using a gene set variation analysis. Considering gender as a covariate for adjustment, we observed significantly higher AR (Fig. 5B) and lower ESR1 (Fig. 5C) filtered regulon activity in *FGFR3*-mutated tumors than in *FGFR3* wild-type tumors in different subtypes in both MIBC and NMIBC, including LumP for ESR1 regulon. We then investigated whether the association of *FGFR3* mutation with higher AR and lower ESR1 activity was linked to FGFR3 activity/expression in our mouse model and BCa cell lines. We observed, contrarily to FGFR3 pathway activation (Fig. 4C), a gradual decrease of ESR1 filtered regulon activity with tumor progression in our FGFR3-induced mouse model (Fig. 5D). We also observed an enrichment of both ESR1 and AR filtered regulons in the DEGs upon FGFR3 siRNA knockdown in human FGFR3-dependent BCa cell lines (Fig. 5E). We further confirmed the inhibition of ESR1 and AR activity by FGFR3-S249C using reporter assays in HEK293FT cells (Fig. 5F). A reporter plasmid comprising the firefly luciferase gene under the control of a promoter containing an AR-response element (PGL4-ARE-X2-PSA-luc) or an ESR1-response element (PsG5-17M-ERE-bGlob-LUC) was coexpressed in HEK293FT cells with a plasmid encoding AR or ESR1, respectively (Fig. 5F, upper panel). FGFR3-S249C expression induced a significantly lower transcriptional activity of AR and ESR1 than transfection with the empty plasmid, in the presence of an AR agonist (2 nM 2-hydroxytestosterone) and phenol red mimicking estrogen, respectively. The FGFR3-S249C–dependent repression of AR and ESR1 transcriptional activity was significantly reduced in the presence of the FGFR inhibitor erdafitinib, demonstrating that the receptor kinase activity was required to modulate hormone receptor activity (Fig. 5F, lower panel). Taken together, our data suggest a causal link between FGFR3 activation and ESR1 activity downregulation but not for AR activity upregulation in *FGFR3*-mutated compared with wild-type tumors. This finding highlights a potential role of an FGFR3-dependent regulation of ESR1 in the sex bias of *FGFR3*-mutated tumors, particularly in the LumP subtype.

4. Discussion

We describe here the first transgenic mouse model demonstrating the tumorigenic role of *FGFR3* mutations in the bladder in vivo. Expression of hFGFR3-S249C in UII-expressing cells induced spontaneous low-grade papillary tumor formation and favored BBN-induced carcinogenesis. In two different transgenic lines, hFGFR3-S249C induced tumorigenesis, indicating an effect of the expression of the

Please cite this article as: M.-J. Shi, J. Fontugne, A. Moreno-Vega et al., FGFR3 Mutational Activation Can Induce Luminal-like Papillary Bladder Tumor Formation and Favors a Male Sex Bias, Eur Urol (2022), https://doi.org/10.1016/j.eururo.2022.09.030

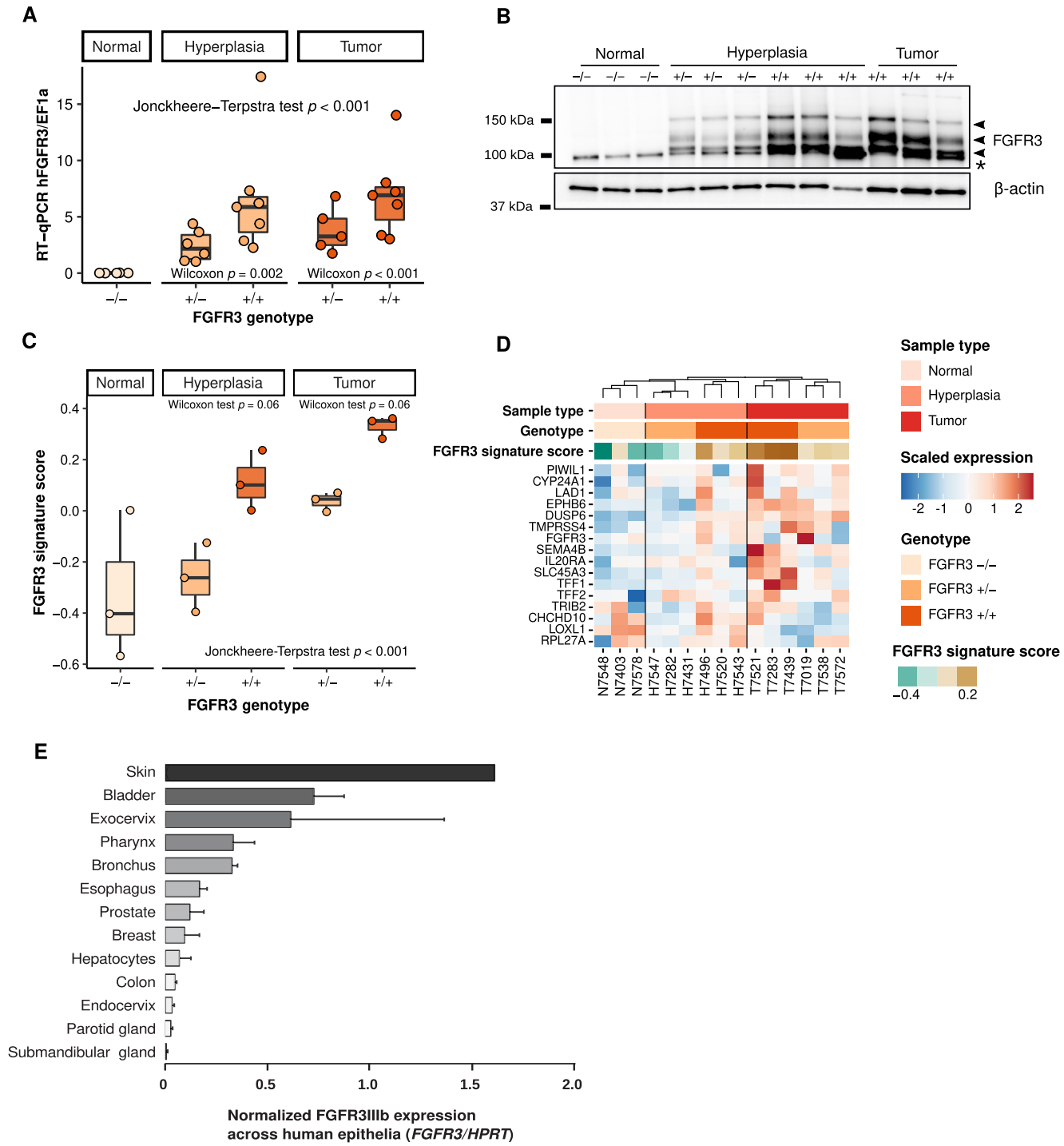

Fig. 4 – *FGFR3*-induced tumor development is dependent on FGFR3 expression levels. (A) *hFGFR3-IIIb* mRNA expression evaluated by RT-qPCR in hyperplastic urothelium or bladder tumors of hFGFR3-S249C homozygous (+/+) or heterozygous (+/–) mice and in normal urothelium of control littermate mice (–/–). Results were normalized using Ef1a expression levels. The statistical difference across all groups was assessed using Jonckheere-Terpstra test and differences between –/+ and +/+ groups were assessed using Wilcoxon rank-sum test. (B) Western blot analysis of hFGFR3 protein levels in normal urothelium of control littermate mice and in hyperplastic urothelium and bladder tumors from either heterozygous (+/–) or homozygous (+/+) hFGFR3-S249C mice. The three bands corresponding to different FGFR3-glycosylation patterns are indicated by an arrow. The asterisk shows a nonspecific band; β-actin was used as a loading control. (C) Comparison of FGFR3 modulation signature scores in normal, hyperplastic, or tumor urothelium from *FGFR3* wild-type mice (normal), or heterozygous and homozygous *hFGFR3*-S249C mice. GSVA-derived FGFR3 signature scores were compared between heterozygous and homozygous hFGFR3-S249C within hyperplastic and tumor tissues using Student *t* tests. The overall increase in *FGFR3* signature scores in tumor development (normal urothelium < hyperplasia < tumor) was confirmed using Jonckheere-Terpstra test. (D) Heatmap of normalized expression values of the FGFR3 modulation signature genes in normal urothelium, hyperplastic urothelium, and tumors. Samples were clustered separately by sample type, grouping genotype in an unsupervised manner. (E) *FGFR3-IIIb* expression levels assessed by RT-qPCR in different normal human epithelia obtained after laser microdissection of surgical biopsies obtained from organ donors. Results are presented as the mean ± SD (*n* = 2 for all samples except skin, *n* = 1, and bladder *n* = 3). FGFR3 = fibroblast growth factor receptor 3; GSVA = gene set variation analysis; RT-qPCR = reverse transcription quantitative polymerase chain reaction; SD = standard deviation.

Please cite this article as: M.-J. Shi, J. Fontugne, A. Moreno-Vega et al., FGFR3 Mutational Activation Can Induce Luminal-like Papillary Bladder Tumor Formation and Favors a Male Sex Bias, Eur Urol (2022), https://doi.org/10.1016/j.eururo.2022.09.030

transgene itself, rather than the alteration of an endogenous key gene resulting from nonspecific transgene insertion. Surprisingly, a mutated FGFR3 has already been targeted to urothelial cells using the same promoter without any spontaneous tumor formation being reported [16–19]. Nonetheless, in some of these studies, mutated receptor expression promoted bladder tumor development when combined with carcinogen exposure [18] or in association

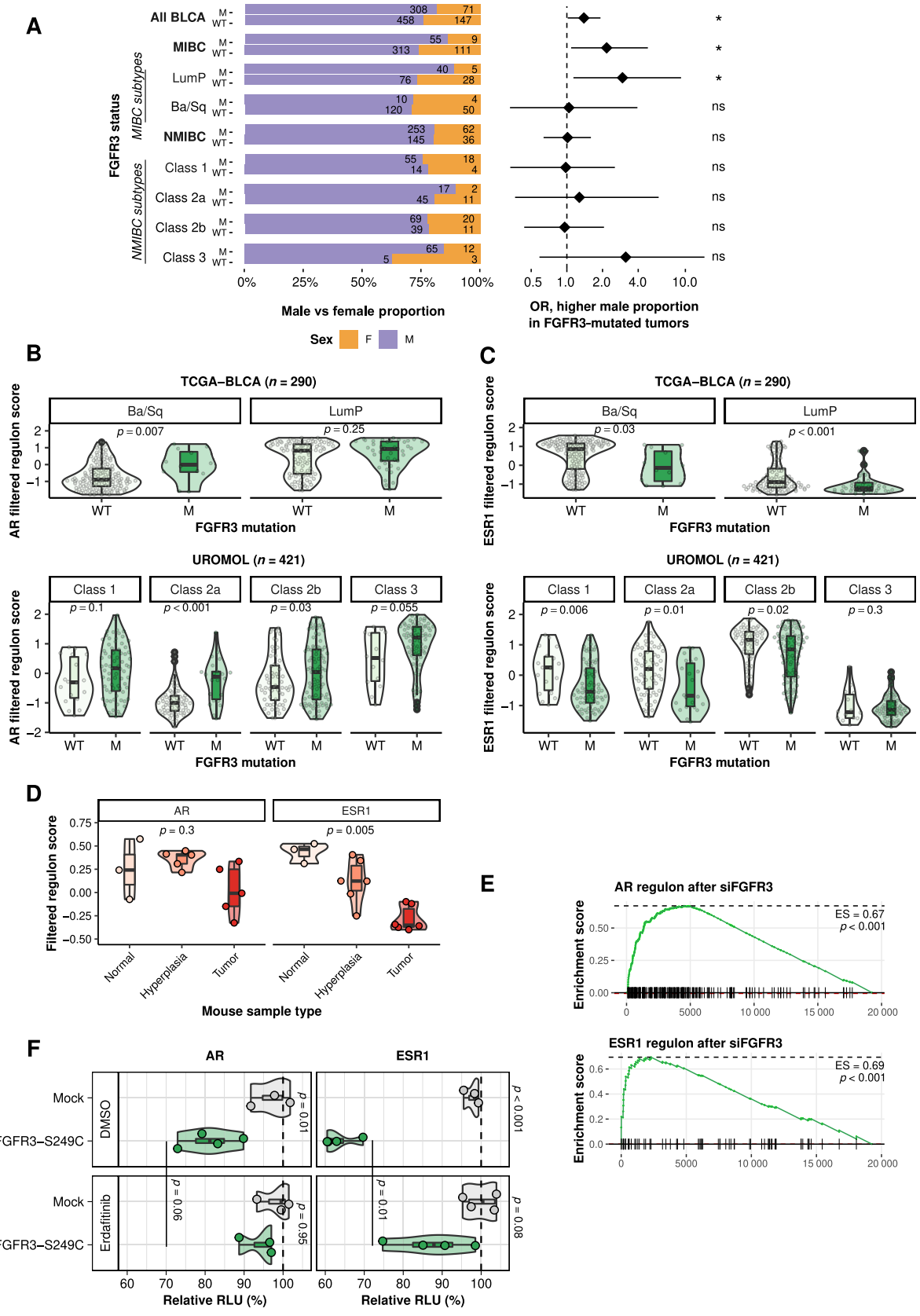

Please cite this article as: M.-J. Shi, J. Fontugne, A. Moreno-Vega et al., FGFR3 Mutational Activation Can Induce Luminal-like Papillary Bladder Tumor Formation and Favors a Male Sex Bias, Eur Urol (2022), https://doi.org/10.1016/j.eururo.2022.09.030

with *Pten* loss [19] or P53/pRB deficiency [17]. The discrepancy between the previously developed GEM models and ours could be linked to the specifically studied *FGFR3* mutation (S249C here and K644E in two previous studies [16,19]) or to the use of an inducible model for FGFR3-S249C expression in other studies [17,18]. We additionally showed that FGFR3-S249C expression levels impact tumor formation frequency, suggesting that lower transgene expression in former GEM models could also account for the absence of tumorigenesis.

FGFR3 mutations are found in very few tumor types. FGFR3-S249C in particular, which is likely induced by APOBEC mutagenesis [8], is rarely found in other APOBEC-related cancer types, such as breast or lung cancers, which suggests that the mutation brings little selective advantage. Our model reveals that a sufficient level of mutant FGFR3 expression is critical to induce tumor formation and that weak FGFR3 expression level in lung and breast normal epithelial cells could explain the absence of *FGFR3* mutation–driven tumor formation in these tissues.

Considering the increasing interest of targeting FGFR3 for BCa treatment, a model resembling the human counterpart at histological, genomic, and transcriptomic levels may have a clinical translational value to evaluate new treatment combinations to prevent resistance. The model we present here is the first immunocompetent model of mutant *FGFR3*–induced low-grade luminal papillary carcinoma, with a tumor microenvironment resembling the human counterpart. *FGFR3*-mutated tumors are non–T cell inflamed and have been associated with a poor immune microenvironment, therefore being less likely to respond to immunotherapy [3,33,34]. Allografts obtained from this model (latency and penetrance of the phenotype will not allow a direct use of the model) should allow an evaluation of combined therapies using both FGFR and checkpoint inhibitors.

Our model should also allow for a better understanding of the signaling pathways activated by FGFR3 in NMIBC. The tumor formation latency and the stage-dependent increase in FGFR3 activation score suggest that a tumor-suppressor pathway and/or a negative regulator of FGFR3 pathways might be activated in normal and hyperplastic urothelia. However, so far our analysis did not reveal such a pathway but confirmed the activation of MYC [14], and highlighted a repression of ER and AR activity by FGFR3. Previous studies using carcinogen-induced mouse models and in vitro transformation assay using normal urothelial cells supported inhibitory functions of ESR1 in urothelial carcinogenesis [35]. Further elucidating whether FGFR3-dependent repression of ESR1 activity could contribute to FGFR3-induced urothelial carcinogenesis and to the male-biased ratio of FGFR3-induced tumors will be of interest. Finally, an additional analysis of the signaling pathway leading to ESR1 repression by FGFR3 is worth further investigation.

5. Conclusions

FGFR3 mutations initiate luminal papillary bladder tumor formation in vivo and favor a male sex bias potentially through inhibition of ESR1 activity. Our findings suggest a potential benefit of FGFR inhibitors in early stages of BCa and premalignant lesions. Our results also suggest that the expression level of FGFR3 in epithelial tissue accounts for the tissue-specificity of FGFR3-driven carcinomas.

Author contributions: Isabelle Bernard-Pierrot had full access to all the data in the study and takes responsibility for the integrity of the data and the accuracy of the data analysis.

Study concept and design: Shi, Fontugne, Moreno-Vega, Meng, Groeneveld, Radvanyi, Bernard-Pierrot.
Acquisition of data: Shi, Fontugne, Moreno-Vega, Meng, Groeneveld, Dufour, Rapinat, Cabel, Krucker, Dunois-Larde, Lepage, Levrel, Dixon, Bernard-Pierrot.
Analysis and interpretation of data: Shi, Fontugne, Moreno-Vega, Meng, Groeneveld, Dufour, Kamoun, Lindskrog, Cabel, Dunois-Larde, Chapeaublanc, Levrel, Radvanyi, Bernard-Pierrot.
Drafting of the manuscript: Shi, Fontugne, Moreno-Vega, Meng, Groeneveld, Bernard-Pierrot.
Critical revision of the manuscript for important intellectual content: All authors.
Statistical analysis: Meng, Groeneveld.
Obtaining funding: Bernard-Pierrot, Radvanyi.
Administrative, technical, or material support: None.

Fig. 5 – *FGFR3* mutations are associated with a higher male sex bias in human tumors and repress *ESR1* transcriptional program. (A) Comparison of sex distribution between *FGFR3*-mutated and wild-type human bladder tumors of different subgroups. Molecular classifications for both NMIBC (UROMOL, CIT) and MIBC (TCGA, CIT), as described previously, in which NMIBC class 3 and MIBC luminal papillary (MIBC LumP) subtypes are known to be enriched for *FGFR3* mutations [3,5,7]. Odds ratios (ORs), corresponding 95% confidence intervals (95% CIs), and Z test–based *p* values were calculated (Materials and methods). OR > 1 represents a higher male proportion in *FGFR3* mutated tumors. (B) AR and (C) ESR1 activity scores for NMIBC and MIBC, calculated using GSVA using AR and ESR1 regulon target gene sets, which were filtered for direct targets identified by CHIP-seq in different tumor types (Supplementary material). The *p* values for comparisons of AR and ESR1 filtered regulon activity between *FGFR3* mutated and wild type by NMIBC or MIBC subtype were calculated using linear regression with gender as a covariate for adjustment. (D) AR and ESR1 filtered regulon scores between UPII-hFGFR3-S249C mouse bladder hyperplasia and tumors compared with control urothelium from littermates. The *p* values were calculated using linear regression with sex as a covariate to control for possible sex bias. (E) GSEA scores for AR (top) and ESR1 (bottom) filtered regulon genes calculated from $\log_2$ fold-change of gene expression upon *FGFR3* knockdown in FGFR3-dependent bladder cancer–derived cell lines (UM-UC-14 [FGFR3-S249C], MGH-U3 [FGFR3-Y375C], and RT112 [FGFR3-TACC3] cells) [8,14]. (F) A reporter plasmid containing the firefly luciferase gene under the control of a promoter containing an AR-response element (PGL4-ARE-X2-PSA-luc) or an ESR1-response element (PsG5-17M-ERE-bGlob-LUC) was coexpressed in HEK293FT cells with a plasmid encoding AR or ESR1, respectively, and a mock pcDNA3 vector or pcDNA encoding hFGFR3-S249C. Cells were treated for 24 h with DMSO or with 100 nM erdafitinib 24 h later, in the presence of 2 nM 2-hydroxytestosterone for an AR reporter assay. Renilla luciferase, expressed under the control of the CMV promoter, was used to normalize the signal (relative light units [RLU]). The data shown are the means ± SD of one representative experiment out of at least three independent ones conducted in quadruplicate. The statistical differences between each condition for AR (left) and ESR1 (right) transcriptional activity were assessed using *t* test. AR = androgen receptor; Ba/Sq = basal/squamous; BLCA = bladder cancer; DMSO = dimethyl sulfoxide; ES = enrichment score; ESR1 = estrogen receptor 1; FGFR3 = fibroblast growth factor receptor 3; GSEA = Gene set enrichment analysis; GSVA = gene set variation analysis; LumP = luminal papillary; M = mutated; MIBC = muscle-invasive bladder cancer; NMIBC = non–muscle-invasive bladder cancer; SD = standard deviation; TCGA = The Cancer Genome Atlas; UII = uroplakin II; WT = wild type.

Please cite this article as: M.-J. Shi, J. Fontugne, A. Moreno-Vega et al., FGFR3 Mutational Activation Can Induce Luminal-like Papillary Bladder Tumor Formation and Favors a Male Sex Bias, Eur Urol (2022), https://doi.org/10.1016/j.eururo.2022.09.030

Supervision: Almeida, De Reynies, Rochel, Dyrskjøt, Allory, Radvanyi, Bernard-Pierrot.
Other: Lebret provided samples and helped with clinical data analysis.

Financial disclosures: Isabelle Bernard-Pierrot certifies that all conflicts of interest, including specific financial interests and relationships and affiliations relevant to the subject matter or materials discussed in the manuscript (eg, employment/affiliation, grants or funding, consultancies, honoraria, stock ownership or options, expert testimony, royalties, or patents filed, received, or pending), are the following: None.

***Funding/Support and role of the sponsor*:** This work was supported by a grant from Ligue Nationale Contre le Cancer (Aura Moreno-Vega, Ming-Jun Shi, Jacqueline Fontugne, Xiang-Yu Meng, Florent Dufour, Claire Dunois-Larde, Elodie Chapeaublanc, May-Linda Lepage, Yves Allory, François Radvanyi, and Isabelle Bernard-Pierrot) as an associated team (Equipe labellisée); the "Carte d'Identité des Tumeurs" program was initiated, developed, and funded by Ligue Nationale Contre le Cancer. Ming-Jun Shi was supported by National Natural Science Foundation of China (NSFC, 82002672). Aura Moreno-Vega was supported by a scholarship from the French Ministry of Research. Xiang-Yu Meng was supported by a fellowship from ITMO Cancer AVIESAN, within the framework of Cancer Plan. Jacqueline Fontugne was supported by the Fondation ARC pour la recherche sur le cancer.

***Data sharing*:** RNAseq data for a cohort of 476 tumors including 460 NMIBC were obtained from ArrayExpress E-MTAB-4321 [5]. RNAseq data and *FGFR3* mutational status for 407 TCGA MIBC were downloaded from cBioPortal for Cancer Genomics: http://www.cbioportal.org/. The microarray for MGH-U3, RT112, and UM-UC-14 cells treated with FGFR3 siRNA are available from GEO (https://www.ncbi.nlm.nih.gov/geo/) under accession number GSE84733 and GSE125547. All other publicly available data used in the current study can be found as described in the Materials and methods. Other data that support the findings of this study are available from the corresponding author upon reasonable request. The microarrays for mouse tumors and hyperplasia and the urothelium from control littermate are available on GEO under reference GSE151888.

Acknowledgments: We thank Xue-Ru Wu and Tung-Tien Sun (NYU) for providing the plasmid with the murine UII promoter, Jeanne-Marie Giraut for the hFGFR3-S249C plasmid construct, Martine Blanche for establishing the UII-hFGFR3-S249C transgenic mice, David Gentien from the genomics platform, and the animal facility members of Institut Curie, particularly Celine Daviaud and Sonia Jannet. We thank Eric Letouzé and Geco (Integragen, Evry, France) for their analysis of mutations and copy number variation in mouse tumors. We thank Ellen Zwarthoff (Erasmus MC Cancer Institute, the Netherlands) for providing FGFR3 mutation status for her cohort of tumors for which transcriptomic data were publicly available. We thank Daniel Metzger (IGBMC, Strasbourg, France) and Francis Vacherot (Paris Est Créteil University, TRePCa, France) for providing plasmids for ESR1 and AR reporter assay, respectively. We thank Daniel Jeffery (Institut Curie, France) for his help in preparing the revised manuscript and the response to reviewers.

Peer Review Summary

Peer Review Summary and Supplementary data to this article can be found online at https://doi.org/10.1016/j.eururo.2022.09.030.

References

[1] Sung H, Ferlay J, Siegel RL, et al. Global cancer statistics 2020: GLOBOCAN estimates of incidence and mortality worldwide for 36 cancers in 185 countries. CA Cancer J Clin 2021;71:209–49.
[2] Kamoun A, de Reyniès A, Allory Y, et al. A consensus molecular classification of muscle-invasive bladder cancer. Eur Urol 2019;77:420–33.
[3] Robertson AG, Kim J, Al-Ahmadie H, et al. Comprehensive molecular characterization of muscle-invasive bladder cancer. Cell 2017;171:540–556.e25.
[4] Sjödahl G, Eriksson P, Liedberg F, Höglund M. Molecular classification of urothelial carcinoma: global mRNA classification versus tumour-cell phenotype classification. J Pathol 2017;242:113–25.
[5] Hedegaard J, Lamy P, Nordentoft I, et al. Comprehensive transcriptional analysis of early-stage urothelial carcinoma. Cancer Cell 2016;30:27–42.
[6] Kim W-J, Kim E-J, Kim S-K, et al. Predictive value of progression-related gene classifier in primary non-muscle invasive bladder cancer. Mol Cancer 2010;9:1–9.
[7] Lindskrog SV, Prip F, Lamy P, et al. An integrated multi-omics analysis identifies prognostic molecular subtypes of non-muscle-invasive bladder cancer. Nat Commun 2021;12:2301.
[8] Shi MJ, Meng XY, Lamy P, et al. APOBEC-mediated mutagenesis as a likely cause of FGFR3 S249C mutation over-representation in bladder cancer. Eur Urol 2019;76:9–13.
[9] Cappellen D, De OC, Ricol D, et al. Frequent activating mutations of FGFR3 in human bladder. Nat Genet 1999;23:18–20.
[10] Porębska N, Latko M, Kucińska M, Zakrzewska M, Otlewski J, Opaliński Ł. Targeting cellular trafficking of fibroblast growth factor receptors as a strategy for selective cancer treatment. J Clin Med 2018;8:7.
[11] Nakanishi Y, Akiyama N, Tsukaguchi T, et al. Mechanism of oncogenic signal activation by the novel fusion kinase FGFR3-BAIAP2L1. Cancer Res 2015;75:123.
[12] Williams SV, Hurst CD, Knowles MA. Oncogenic FGFR3 gene fusions in bladder cancer. Hum Mol Genet 2013;22:795–803.
[13] Bernard-Pierrot I, Brams A, Dunois-Lardé C, et al. Oncogenic properties of the mutated forms of fibroblast growth factor receptor 3b. Carcinogenesis 2006;27:740–7.
[14] Mahe M, Dufour F, Neyret-Kahn H, et al. An FGFR3/MYC positive feedback loop provides new opportunities for targeted therapies in bladder cancers. EMBO Mol Med 2018;10:e8163.
[15] Loriot Y, Necchi A, Park SH, et al. Erdafitinib in locally advanced or metastatic urothelial carcinoma. N Engl J Med 2019;381:338–48.
[16] Ahmad I, Singh LB, Foth M, et al. K-Ras and b-catenin mutations cooperate with Fgfr3 mutations in mice to promote tumorigenesis in the skin and lung, but not in the bladder. Dis Model Mech 2011;4:548–55.
[17] Zhou H, He F, Mendelsohn CL, Tang MS, Huang C, Wu XR. FGFR3b extracellular loop mutation lacks tumorigenicity in vivo but collaborates with p53/pRB deficiency to induce high-grade papillary urothelial carcinoma. Sci Rep 2016;6:1–11.
[18] Foth M, Ismail NFB, Kung JSC, et al. FGFR3 mutation increases bladder tumourigenesis by suppressing acute inflammation. J Pathol 2018;246:331–43.
[19] Foth M, Ahmad I, Van Rhijn BWG, et al. Fibroblast growth factor receptor 3 activation plays a causative role in urothelial cancer pathogenesis in cooperation with Pten loss in mice. J Pathol 2014;233:148–58.
[20] Zhang ZT, Pak J, Shapiro E, Sun TT, Wu XR. Urothelium-specific expression of an oncogene in transgenic mice induced the formation of carcinoma in situ and invasive transitional cell carcinoma. Cancer Res 1999;59:3512–7.
[21] Rebouissou S, Bernard-Pierrot I, de Reyniès A, et al. EGFR as a potential therapeutic target for a subset of muscle-invasive bladder cancers presenting a basal-like phenotype. Sci Transl Med 2014;6:244ra91.
[22] Saito R, Smith CC, Utsumi T, et al. Molecular subtype-specific immunocompetent models of high-grade urothelial carcinoma reveal differential neoantigen expression and response to immunotherapy. Cancer Res 2018;78:3954–68.
[23] Fantini D, Glaser AP, Rimar KJ, et al. A Carcinogen-induced mouse model recapitulates the molecular alterations of human muscle invasive bladder cancer. Oncogene 2018;37:1911–25.

Please cite this article as: M.-J. Shi, J. Fontugne, A. Moreno-Vega et al., FGFR3 Mutational Activation Can Induce Luminal-like Papillary Bladder Tumor Formation and Favors a Male Sex Bias, Eur Urol (2022), https://doi.org/10.1016/j.eururo.2022.09.030

[24] Biton A, Bernard-Pierrot I, Lou Y, et al. Independent component analysis uncovers the landscape of the bladder tumor transcriptome and reveals insights into luminal and basal subtypes. Cell Rep 2014;9:1235–45.
[25] Damrauer JS, Hoadley KA, Chism DD, et al. Intrinsic subtypes of high-grade bladder cancer reflect the hallmarks of breast cancer biology. PNAS 2014;111:3110–5.
[26] Becht E, Giraldo NA, Lacroix L, et al. Estimating the population abundance of tissue-infiltrating immune and stromal cell populations using gene expression. Genome Biol 2016;17:1–20.
[27] Logié A, Dunois-Lardé C, Rosty C, et al. Activating mutations of the tyrosine kinase receptor FGFR3 are associated with benign skin tumors in mice and humans. Hum Mol Genet 2005;14:1153–60.
[28] Hafner C, Van Oers JMM, Vogt T, et al. Mosaicism of activating FGFR3 mutations in human skin causes epidermal nevi. J Clin Invest 2006;116:2201–7.
[29] Rosty C, Aubriot MH, Cappellen D, et al. Clinical and biological characteristics of cervical neoplasias with FGFR3 mutation. Mol Cancer 2005;4:2–9.
[30] Yang A, Cannataro VL, Townsend JP. Re: Ming-Jun Shi, Xiang-Yu Meng, Philippe Lamy, et al. APOBEC-mediated mutagenesis as a likely cause of FGFR3 S249C mutation over-representation in bladder cancer. Eur Urol 2019;76:9–13. Eur Urol 2020;77:e24–5.
[31] Shi MJ, Meng XY, Chen CL, et al. Reply to Alexander Yang, Vincent L. Cannataro, Jeffrey P. Townsend's Letter to the Editor, re: Ming-Jun Shi, Xiang-Yu Meng, Philippe Lamy, et al. APOBEC-mediated mutagenesis as, a likely cause of FGFR3 S249C mutation over-representation in bladder cancer. Eur Urol 2020;77:e26–7.
[32] Lin C, Yin Y, Stemler K, et al. Constitutive β-catenin activation induces male-specific tumorigenesis in the bladder urothelium. Cancer Res 2013;73:5914–25.
[33] Kardos J, Chai S, Mose LE, et al. Claudin-low bladder tumors are immune infiltrated and actively immune suppressed. JCI Insight 2016;1:e85902.
[34] Sweis RF, Spranger S, Bao R, et al. Molecular drivers of the non-T cell-inflamed tumor microenvironment in urothelial bladder cancer. Cancer Immunol Res 2016;4:563–8.
[35] Goto T, Miyamoto H. The role of estrogen receptors in urothelial cancer. Front Endocrinol (Lausanne) 2021;12:643870.

Please cite this article as: M.-J. Shi, J. Fontugne, A. Moreno-Vega et al., FGFR3 Mutational Activation Can Induce Luminal-like Papillary Bladder Tumor Formation and Favors a Male Sex Bias, Eur Urol (2022), https://doi.org/10.1016/j.eururo.2022.09.030